

GAMMA RAYS FROM ROTATION-POWERED PULSARS

ALICE K. HARDING

Code 661, NASA Goddard Space Flight Center, Greenbelt, MD 20771

The seven known gamma-ray pulsars represent a very small fraction of the more than 1000 presently known radio pulsars, yet they can give us valuable information about pulsar particle acceleration and energetics. Although the theory of acceleration and high-energy emission in pulsars has been studied for over 25 years, the origin of the pulsed gamma rays is a question that remains unanswered. Characteristics of the pulsars detected by the Compton Gamma-Ray Observatory could not clearly distinguish between an emission site at the magnetic poles (polar cap models) and emission from the outer magnetosphere (outer gap models). There are also a number of theoretical issues in both type of model, which have yet to be resolved. The two types of models make contrasting predictions for the numbers of radio-loud and radio-quiet gamma-ray pulsars and of their spectral characteristics. GLAST will probably detect at least 50 radio-selected pulsars and possibly many more radio-quiet pulsars. With this large sample, it will be possible to fully test the model predictions and finally resolve this longstanding question.

1 Introduction

The Compton Gamma-Ray Observatory (CGRO), which ended its spectacularly successful mission in June 2000, provided a wealth of new data on isolated, rotation powered pulsars. While that data went a long way in constraining emission models, it was not enough to define the location or mechanisms of the high energy pulsed emission and ultimately, of the particle acceleration. Meanwhile, as we have been waiting for the launch of the next γ -ray telescopes, Integral, AGILE and GLAST, there have been a large number of new pulsars detected at radio and X-ray wavelengths by the Parkes Multibeam survey¹ and by the Chandra X-ray Observatory. Many of these are young and energetic pulsars, prime γ -ray pulsar candidates and many of them lie in or near the error boxes of unidentified γ -ray sources². Observations of these sources at γ -ray wavelengths promise a harvest of new data for the study of high-energy emission from isolated pulsars.

2 Summary of Observations

During its nine-year mission, observations by CGRO increased the number of known γ -ray pulsars from two to seven. In addition, EGRET made four “candidate” detections with somewhat lower significance, including the millisecond pulsar PSR J0218+4232³. Table 1 lists the known γ -ray pulsars together with the rotation-powered X-ray pulsars. There are three main groups of sources in Table 1: pulsars detected only in X rays, those detected in X rays and radio and those detected in γ rays, X rays and radio. One interesting and important question is the number of high-energy pulsars that are radio quiet. Since it is generally believed that radio emission origi-

nates near the polar caps of the neutron star, lack of detection in the radio (if due to unfavorable beaming) would strongly constrain the location and geometry of the high-energy emission. All of the known γ -ray pulsars are radio-loud with the possible exception of Geminga, which has unconfirmed reports of weak radio emission⁴. But they are also radio selected, since EGRET was not capable of independent period searches. The ten radio-loud X-ray pulsars which were not detected as γ -ray pulsars fall into several categories. The first five are millisecond pulsars (only one γ -ray pulsar is a ms pulsar), the last three are young pulsars in supernova remnants, too recently discovered to have provided concurrent ephemerides for CGRO detections, PSR B1929+10 is a 10^7 yr old pulsar with only thermal X-ray emission and PSR B0540-69 is a young pulsar in the LMC. Finally, the seven pulsars detected only in X rays are a collection of all categories and may be truly radio quiet. However, it has recently become apparent that lack of detection by even the most sensitive radio surveys is not proof that the pulsar is radio quiet. J11245916^{5,6} and J0205+6449^{7,8} were recently discovered to be very weak radio pulsars only after long, pointed observations. The unexpected finding that these young pulsars have extremely low radio luminosities is raising new questions about the radio luminosity function and its implications for the neutron star birthrate.

Figure 1 plots the known radio and γ -ray pulsars as a function of their period, P , and period derivative, \dot{P} . The γ -ray pulsars reside in the upper-left corner of the radio pulsar population, and with the exception of the millisecond pulsar J0218+4232, all have ages less than 10^6 yr. Also shown are the sixteen radio pulsars associated with EGRET unidentified sources. It is remarkable that with one exception, all have ages less than 10^5 yr, suggesting that some real associations of the γ -ray emission with emission from the pulsars or their nebulae is likely.

A pattern which emerged from the γ -ray pulsar light curves measured by CGRO was that, with the one exception of PSR1509-58, all have double-peaked pulses with interpeak emission. This strongly suggests that we are observing emission associated with just one of the magnetic poles and that the emission pattern is a hollow cone or wide fan beam. Most of the pulsars detected only at X-ray energies, by contrast, have broad single-peaked pulses. In most cases, the radio pulses lead the γ -ray pulses in phase rather than being coincident. Another strong pattern identified in the CGRO pulsars was a correlation between high-energy luminosity and the quantity $P^{-3/2}\dot{P}^{1/2}$, where P and \dot{P} are the pulsar rotation period and period derivative, respectively. For a pure dipole field, this quantity is proportional to the polar cap current, the voltage across open field lines and $\dot{E}_{\text{rot}}^{1/2}$, where \dot{E}_{rot} is the spin-down luminosity. Thus the γ -ray luminosity seems to be closely tied to the primary particle acceleration of the pulsar.

The broad-band spectra from radio to TeV energies of the seven confirmed CGRO γ -ray pulsars⁹ show that the emission power in these sources peaks in the hard X-ray or γ -ray part of the spectrum. The spectra of all the CGRO pulsars have clear high-energy turnovers since none have detected pulsed emission above 20 GeV. Three pulsars, Vela, Crab and Geminga, have spectral turnovers in the EGRET range, around 5 GeV and one, PSR1509-58, has a sharp turnover in the COMPTEL range around 10 MeV. Below the turnovers, there is a trend of increasing spectral hardness with dipole spin-down age, $\tau = P/2\dot{P}$. In the middle-aged and older pulsars, a thermal component in the soft X-ray band is visible above the falling power-law continuum. This component is probably present also in young pulsars but hidden beneath the strong power-law.

3 Emission Models and Predictions

Particle acceleration inside the pulsar magnetosphere gives rise to pulsed non-thermal radiation. Rotating, magnetized neutron stars are natural unipolar inductors, generating huge $\mathbf{v}\times\mathbf{B}$ electric fields. However, these fields are capable of pulling charges out of the star against the force of gravity and it is believed that the resulting charge density that builds up in a neutron star

Table 1: High-Energy Pulsars

PSR	P (ms)	\dot{P} (10^{-15}s s^{-1})	Gamma-ray	X-Ray	Radio	SNR/Name
B0531+21	33.0	422.0	X	X	X	Crab
B1509-58	150.0	1540.0	X	X	X	MSH15-52
B0833-45	89.0	124.0	X	X	X	Vela
B1706-44	102.0	92.2	X	X	X	
B1951+32	39.5	5.9	X	X	X	CTB 80
J0633+1746	237.0	11.4	X	X	(X)	Geminga
B1055-52	197.0	5.8	X	X	X	
B0656+14	384.0	55.0	(X)	X	X	
J0218+4232	2.3	8.3E-05	(X)	X	X	
B1046-58	124.0	103.6	(X)	X	X	
J2229+6114	51.6	78.3	(X)	X	X	
B1957+21	1.60	1.1E-04		X	X	
J0437+4715	5.70	5.7E-05		X	X	
J0030+0451	4.86	1.0E-05		X	X	
J2124-3358	4.93	2.1E-05		X	X	
B1821-24	3.05	1.6E-03		X	X	
B1929+10	226.0	1.2		X	X	
B0540-69	50.0	479.0		X	X	
J1420-6048	68.0	83.0		X	X	Kookaburra
J1124-5916	136.0	740.0		X	X	G292.0+1.8
J0205+6449	65.7	193.0		X	X	3C 58
J0537-6910	16.1	51.2		X		N147B
J0635+0533	33.9	*		X		
J1811-1926	64.7	44.0		X		G11.2-0.3
J1846-0258	324.0	7097.1		X		Kes75
J161730-50	69.0	140.0		X		RCW 103
J0822-43	75.3	149.0		X		Puppis A
1E1207.4-52	424.0			X		PKS1209-52

magnetosphere is able to short out the electric field parallel to the magnetic field (E_{\parallel})(thus allowing the field to corotate with the star) everywhere except at a few locations. Two possible sites where $\mathbf{E} \cdot \mathbf{B} \neq 0$, and strong E_{\parallel} may develop to accelerate particles, have given rise to two classes of high energy emission models: polar cap models, where the acceleration and radiation occur at the magnetic poles close to the neutron star surface, and outer gap models, where these processes occur in the outer magnetosphere.

3.1 Polar cap

Polar cap models^{10,11} advocate that particle acceleration occurs near the neutron star surface and that γ -rays result from a curvature radiation or inverse Compton induced pair cascade in a strong magnetic field. There is some variation among polar cap models, with the primary division being whether or not there is free emission of particles from the neutron star surface. The subclass of polar cap models based on free emission of particles of either sign, called space-charge limited flow models, assumes that the surface temperature of the neutron star (many of which have now been measured in the range $T \sim 10^5 - 10^6$ K) exceeds the ion and electron thermal

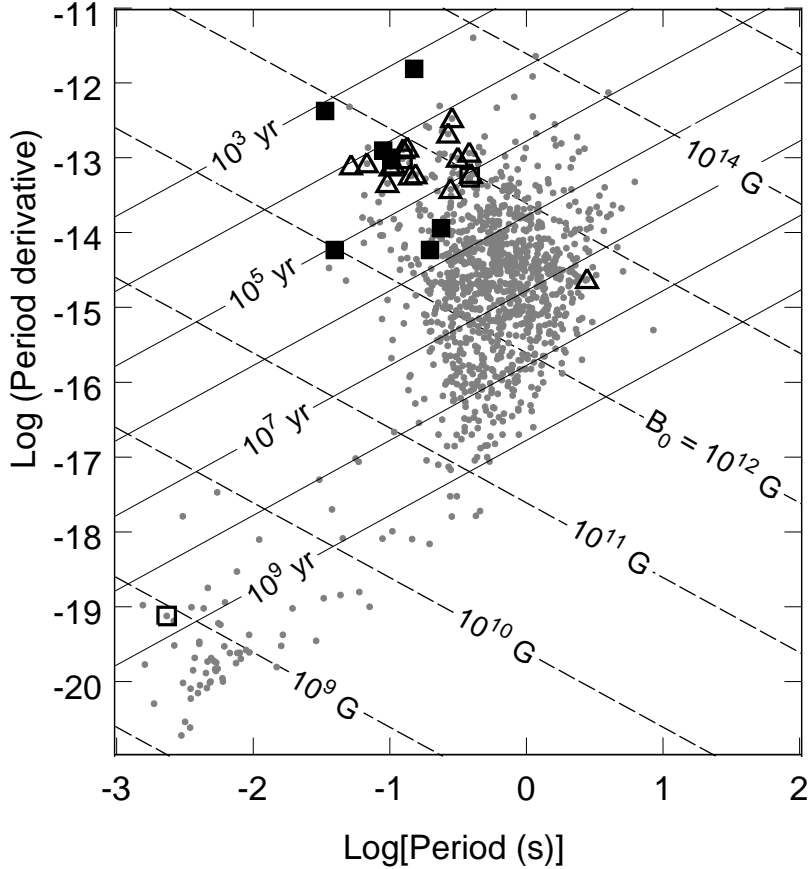


Figure 1: Plot of period-derivative \dot{P} vs. period P of radio pulsars (gray dots) from the ATNF Pulsar Catalog (<http://www.atnf.csiro.au/pulsar/>) with confirmed (solid squares) and candidate (open squares) γ -ray pulsars. Also plotted are radio pulsars in EGRET unidentified source error boxes (open triangles). Solid diagonal lines indicate spin-down age, $\tau = P/2\dot{P}$.

emission temperatures. Although $E_{\parallel} = 0$ at the neutron star surface in these models, the space charge along open field lines above the surface falls short of the corotation charge, due to the curvature of the field¹² or to general relativistic inertial frame dragging¹³. The E_{\parallel} generated by the charge deficit accelerates particles, which radiate inverse Compton (IC) photons (at particle Lorentz factors $\gamma \sim 10^2 - 10^6$) and curvature (CR) photons (at Lorentz factors $\gamma \gtrsim 10^6$). Recent studies^{14,15} have found that virtually *all* pulsars can produce IC radiation, by scattering thermal X rays from the NS surface, at high enough energies to produce pairs. The IC emission is mostly resonant scattering in high-field pulsars and non-resonant scattering in older and weaker field pulsars. Because lower Lorentz factors are required to produce pairs through IC emission, an IC pair formation front (PFF) will form first, close to the surface. However, it is found¹⁵ that the IC pair formation fronts do not produce sufficient pairs to screen the E_{\parallel} completely, thus allowing acceleration to the Lorentz factors $\sim 10^7$ sufficient to produce a CR PFF, where there are sufficient pairs to completely screen the E_{\parallel} . The CR pair front will therefore limit the particle acceleration voltage and determine the high-energy emission luminosity.

It has been realized for some time that only younger pulsars are capable of producing pairs

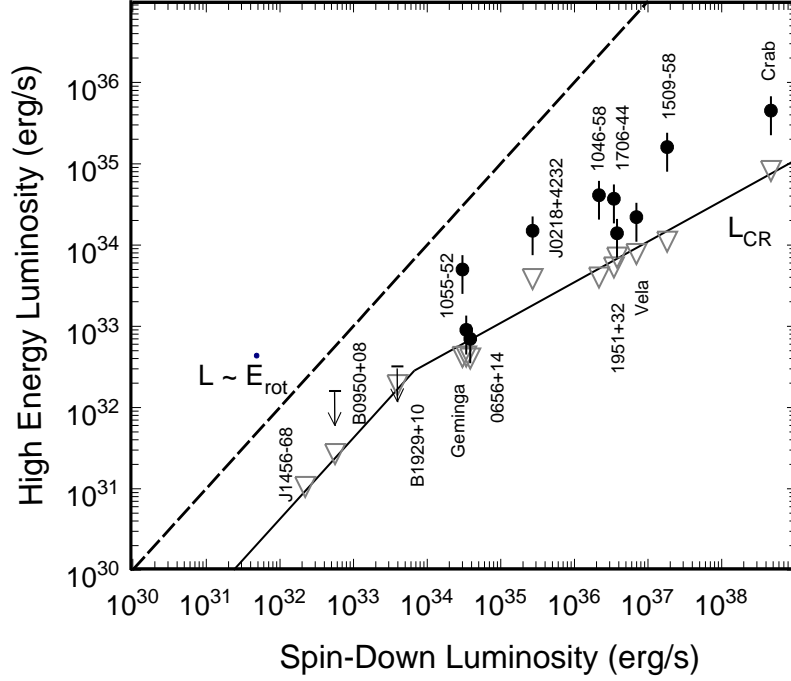


Figure 2: Predicted and observed high energy luminosity vs. spin-down luminosity. The solid curve is the theoretical prediction from eq. (2). The solid circles are the luminosities of the detected γ -ray pulsars¹⁷, derived from detected fluxes above 1 eV assuming a 1 sr. solid angle. The upper limits are for > 100 MeV from¹⁸. The open triangles are predicted luminosities for the detected pulsars.

(and pair cascades) through CR emission in dipole magnetic fields¹². These pulsars with

$$\dot{E}_{\text{rot}} > \dot{E}_{\text{rot,break}} = 5 \times 10^{33} P^{-1/2} \text{ erg} \cdot \text{s}^{-1}. \quad (1)$$

will have screened E_{\parallel} , so that the acceleration voltage Φ is nearly independent^{15,16} of the period and surface magnetic field, B_0 . Pulsars having spin-down luminosity $\dot{E}_{\text{rot}} < \dot{E}_{\text{rot,break}}$ will not produce CR pairs to screen E_{\parallel} , so that the acceleration voltage will be limited only by the saturation due to the geometry of the polar cap and this *does* depend on P and B_0 . The bolometric luminosity is $L_{\text{CR}} \simeq \epsilon \Phi \dot{n}_{\text{prim}} \simeq \epsilon \Phi n_{\text{GJ}} \pi R_{\text{PC}}^2 c$, where $\dot{n}_{\text{prim}} \propto \dot{E}_{\text{rot}}^{1/2}$ is the primary PC current, n_{GJ} is the Goldreich-Julian density, R_{PC} is the polar cap radius, and ϵ is a radiation efficiency. We thus have the luminosity prediction

$$L_{\text{CR}} = \begin{cases} \epsilon 10^{16} (\text{erg/s})^{1/2} \dot{E}_{\text{rot}}^{1/2} P^{1/4} B_{12}^{-1/7} & \dot{E}_{\text{rot}} > \dot{E}_{\text{rot,break}} \\ \epsilon \frac{3}{4} \kappa (1 - \kappa) \dot{E}_{\text{rot}} & \dot{E}_{\text{rot}} < \dot{E}_{\text{rot,break}} \end{cases} \quad (2)$$

for PC space-charge limited flow acceleration¹⁶, where $\kappa = r_g I / MR^3 \simeq 0.14$, and r_g is the gravitational radius of a NS of mass M , and I and R are the stellar moment of inertia and radius, respectively. The above expression is valid for surface fields $B_0 \lesssim 5 \times 10^{12}$ G. Figure 2 shows the predicted luminosity from Eqn (2), assuming $\epsilon = 0.5$, and the luminosities of the observed γ -ray pulsars. The break from $L_{\text{CR}} \propto \dot{E}_{\text{rot}}$ to $L_{\text{CR}} \propto \dot{E}_{\text{rot}}^{1/2}$ is predicted to occur for luminosities just below that of the detected γ -ray pulsars.

Polar cap models predict that the γ -ray spectra cut off very sharply (as a “super-exponential”) due to one-photon pair production attenuation, at the pair escape energy¹⁹, i.e. the highest energy at which photons emitted at a given location can escape the magnetosphere without pair

producing. A rough estimate of this cutoff energy, assuming emission along the polar cap outer rim, $\theta_{\text{PC}} \simeq (2\pi r/cP)^{1/2}$, at radius r , is

$$E_c \sim 2 \text{ GeV } P^{1/2} \left(\frac{r}{R}\right)^{1/2} \max \left\{ 0.1, B_{0,12}^{-1} \left(\frac{r}{R}\right)^3 \right\} \quad (3)$$

where $B_{0,12}$ is the surface magnetic field in units of 10^{12} G. At all but the highest fields there is a prediction that the spectral cutoff energy should be inversely proportional to surface field strength, or $B_0 = 6.4 \times 10^7 P\dot{P}^{1/2}$ G for a dipole field. In fields above $\sim 2 \times 10^{13}$ G, photon splitting, in which a single photon splits into two lower energy photons, becomes the dominant attenuation process and lowers the photon escape energy^{19,20}. The observed cutoff energies of eight γ -ray pulsars seem to increase with decreasing surface field²¹, although a larger number of measurements are needed to confirm this trend.

According to Eqn (2), millisecond pulsars should have detectable high-energy emission. However only one, PSR J0218+4232, has been detected in γ rays by EGRET³. But the polar cap particle acceleration in millisecond pulsars will be limited by curvature radiation reaction^{22,16} so that the CR emission spectrum will be quite hard (photon index $-2/3$). Because ms pulsars have surface fields of only $B_0 \sim 10^8 - 10^{10}$ G, the spectral cutoff will not be caused by magnetic pair production at an energy of a few GeV, but will occur at the cutoff of the CR spectrum, causing the νF_ν spectrum to peak at 50-100 GeV energies²³. There may be a second spectral component at X-ray energies from IC pair cascades. This may explain why many millisecond pulsars detected at X-ray energies are not detectable by EGRET, but may be visible to air Cherenkov telescopes having thresholds below 100 GeV.

3.2 Outer gap

Outer-gap models^{24,25} assume that acceleration occurs in vacuum gaps along null charge surfaces in the outer magnetosphere and that γ rays result from photon-photon pair production-induced cascades. The gaps arise because charges escaping through the light cylinder along open field lines above the null charge surface cannot be replenished from below. Pairs from the polar cap cascades, which flow out along all the open field lines, will undoubtedly pollute the outer gaps to some extent (and vice versa), but this effect has yet to be investigated. The electron-positron pairs needed to provide the current in the outer gaps are produced by photon-photon pair production. In young Crab-like pulsars, the pairs are produced by CR photons from the primary particles interacting with non-thermal synchrotron X-rays from the same pairs. In older Vela-like pulsars, where non-thermal X-ray emission is much lower, the pairs are assumed to come from interaction of primary particles with thermal X-rays from the neutron star surface. Some of the accelerated pairs flow downward to heat the surface and maintain the required thermal X-ray emission. The modern outer gap Vela-type models^{25,26} all adopt this picture. Although there seems to be agreement on the radiation processes involved in the outer gap, the full geometry of the gap is still not solved. Two approaches to such a solution are currently underway, but neither is near to defining the complete three-dimensional gap geometry. One group^{25,27} solves the 1D Poisson equation perpendicular to the magnetic field lines, resulting in a gap geometry for young pulsars that is a long, thin sheet bounded by the last open field line. The other group²⁸ obtains solutions to the 1D Poisson equation along the magnetic field (assuming a gap width across field lines) and finds that the gap is limited parallel to the field by pair creation. The actual gap geometry is probably somewhere in between (see Figure 3). The long narrow outer gap geometry of Yadigaroglu & Romani²⁹ and Cheng et al.²⁷, which has been so successful in reproducing the observed double-peaked pulse profiles needs to be re-examined to also explore gap closure along the field.

When the high-energy photons are emitted in the outer magnetosphere, where the local magnetic field is orders of magnitude lower than the surface field, one-photon pair production plays no role in either the pair cascade or the spectral attenuation. In this case the high-energy cutoffs in the photon spectrum come from the upper limit of the accelerated particle spectrum, due to radiation reaction. The shape of the cutoff is thus a simple exponential, more gradual than in polar cap model spectra. Due to the large errors of the EGRET data points above 1 GeV, the measurements at present do not definitely discriminate between model spectra. GLAST should have the energy resolution and dynamic range to measure the shape of the cutoffs seen by EGRET and should be able to rule out either the simple exponential or super-exponential shape. In addition, GLAST will detect enough γ -ray pulsars with different field strengths to look for a correlation between surface field strength and cutoff energy.

Outer gap models predict an emission component at TeV energies due to inverse Compton scattering by gap-accelerated particles. TeV photons should escape from the outer gaps of pulsars with even strong surface fields and this component is thus expected to be observable in many pulsars. The original predictions of Cheng et al.²⁴ were not verified by observations of ground-based detectors^{30,31}, requiring a revision of the Vela-like model³². However, even later models which predicted lower TeV fluxes²⁵ are above CANGAROO upper limits on pulsed emission from Vela³³. The most recent outer gap models^{28,35}, have predicted TeV inverse-Compton fluxes which are below the present observational upper limits, but which should be detectable with the next generation of TeV detectors. Unfortunately, while a TeV emission component is an essential prediction of all outer gap models, the inverse Compton flux level depends on the pulsed emission spectrum in the infra-red (IR) band which is notoriously difficult to measure in most pulsars.

Unlike in polar cap models, pair production in outer gap models is essential to the production of the high energy emission: it allows the current to flow and particle acceleration to take place in the gap. Beyond a death line in period-magnetic field space, and well before the traditional radio-pulsar death line, pairs cannot close the outer gap and the pulsar cannot emit high energy radiation. This outer gap death line for γ -ray pulsars³⁴ falls around $P = 0.3$ s for $B \sim 10^{12}$ G. Geminga is very close to the outer gap death line and recent self-consistent models³⁵ have difficulty accounting for GeV γ -rays from pulsars of this age. Polar cap models, on the other hand, predict that all pulsars are capable of γ -ray emission at some level, so that detection as a radio-loud γ -ray pulsar is thus a matter of sensitivity. Detection of pulsars with periods much exceeding that of Geminga would thus be strong evidence in favor of polar cap models.

4 Geometry, Population Statistics and Radio-Quiet Pulsars

In polar cap models, the γ -ray and radio emission are physically connected, since the electron-positron pairs from the PC cascades are thought to be a necessary ingredient for coherent radio radiation. However, the relative geometry of the two emission regions is not very constrained from observation. A possible scheme for the geometry of the radio and high-energy emission beams is shown in Figure 3. Models for radio emission morphology^{36,37} include core and conal components, emitted within a radius of about ten stellar radii from the surface. If the PC γ -ray cone emission occurs at a lower altitude than the radio emission, as would be expected, then the leading edge of the radio cone would lead the first γ -ray peak. The trailing edge of the radio conal emission would then have to be undetected in the CGRO pulsars. This type of radio geometry for young pulsars was suggested by Manchester³⁸ and there is indeed a class of pulsars with one-sided radio conal emission³⁷. Another requirement on the geometry of polar cap γ -ray emission is that the inclination angle be comparable to or smaller than the size of the γ -ray emission beam. Since the high-energy emission beam is comparable to the angle of the open field lines, $\theta_{PC} \sim (\Omega r/c)^{1/2}$, this requirement is very restrictive unless the emission radius, r , is

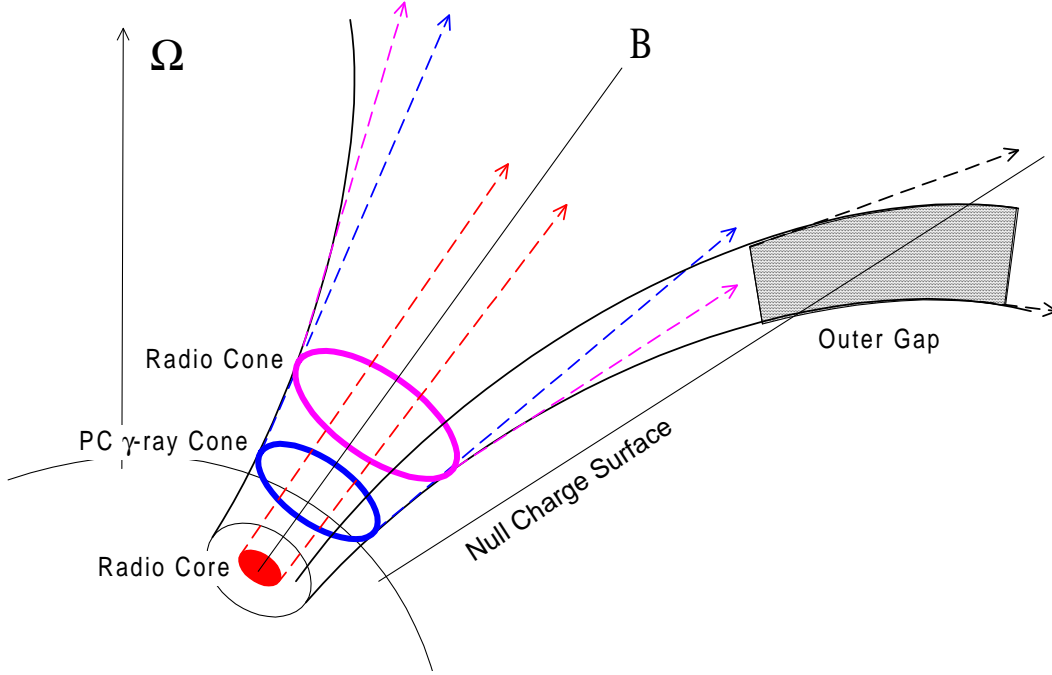


Figure 3: Cartoon of polar cap, outer gap and radio beams (not necessarily to scale). The outer gap is shown as a 2D projection, so that the full 3D extent of the gap and beam is not represented.

at least several stellar radii¹⁰.

High energy emission in the outer gap is generally radiated in a different direction from the radio emission, which allows these models to account for the observed phase offsets of the radio and γ -ray pulses. At the same time, there will be fewer radio- γ -ray coincidences and thus a larger number of radio-quiet γ -ray pulsars. In Romani & Yadigaroglu’s³⁹ geometrical outer gap model, the observed radio emission originates from the magnetic pole opposite to the one connected to the visible outer gap. Many observer lines-of-sight miss the radio beam but intersect the outer-gap γ -ray beam, having a much larger solid angle. When the line-of-sight does intersect both, the radio pulse leads the γ -ray pulse, as is observed in most γ -ray pulsars.

The emission geometry greatly influences the predicted numbers of radio-loud and radio-quiet γ -ray pulsars. Polar cap γ -ray emission is expected to have a much higher observational correlation than outer-gap emission with the radio emission. Simulations of the radio and γ -ray pulsar populations in both models confirm this. Although there are significant variations in the numbers of predicted γ -ray pulsars due to different model assumptions in the various studies, outer gap models clearly predict a much larger ratio of radio-quiet to radio-loud γ -ray pulsars. Polar cap model simulations⁴⁰ find that EGRET should have detected many fewer radio-quiet than radio-loud pulsars, while outer gap model simulations^{29,41} claim that many of the 40-60 EGRET unidentified sources at low latitudes are radio-quiet pulsars. However, pulsars are “radio-quiet” in PC models primarily because their flux is below the sensitive limit of present radio surveys but in outer gap models primarily because the radio emission is beamed away from us. The polar cap model simulations⁴⁰ predict that GLAST should detect slightly more radio-quiet than radio-loud pulsars as point sources. Although GLAST will have the capability to detect pulsed γ -ray emission, the required sensitivity is much higher, about equal to the EGRET point source sensitivity. Thus, only about 10% of the radio-quiet sources will have detected γ -ray pulsations. The outer gap simulations⁴¹ predict that GLAST may detect 13

times as many radio-quiet as radio-loud pulsars as point sources, with the detected number of radio-quiet pulsars equaling the present radio pulsar population! This would have profound consequences for neutron star evolution and supernova rates in the galaxy.

Another possible population of radio-quiet γ -ray pulsars has been suggested⁴². According to the polar cap model¹⁰, γ -ray emission occurs throughout the entire pulse phase. Primary electrons that initiate pair cascades at low altitude continue to radiate curvature emission on open field lines to high altitudes beyond the cascade region, producing a lower level of softer off-beam emission. Due to the flaring of the dipole field lines, this emission may be seen over a large solid angle, far exceeding that of the main γ -ray and radio beams. It is therefore quite probable to see the off-beam γ -ray emission and miss the radio beam. But since it is much less luminous than the on-beam emission, off-beam emission will be detectable only in nearby sources. EGRET detected a population of unidentified γ -ray sources correlated with the Gould Belt⁴³, a young star cluster only 100 – 300 pc away, and recent simulations of pulsars in the Gould Belt^{44,2} suggest that such off-beam γ -ray emission might plausibly account for a significant fraction of these sources.

5 Prospects for the Future

Our window on the γ -ray universe from space will open again soon with the launch of Integral⁴⁵ in October 2002, AGILE⁴⁶ in 2003 and ultimately GLAST² in 2006. Searches for pulsed γ rays in EGRET unidentified source error boxes with simultaneous timing of the new radio pulsars associated with these sources may finally provide some counterparts. Searching for γ -ray emission from the recently discovered X-ray pulsars inside young supernova remnants may also be fruitful. Although it is only slightly more sensitive than EGRET, AGILE may significantly add to the γ -ray pulsar population due to the tripling of the radio pulsar population since the death of CGRO. With its better sensitivity at energies above 1 GeV, AGILE will be able to improve measurements of the spectral cutoffs detected by EGRET and discriminate between emission models. GLAST will detect at least an order of magnitude more radio-loud pulsars and many more radio-quiet pulsars. It will, for the first time, be capable of doing blind period searches in about 10% of the source population in the plane and all of the source population detected by EGRET in the Gould Belt. Meanwhile, more sensitive ground-based air Cherenkov telescope⁴⁷ may be able to detect the pulsed inverse-Compton emission around 1 TeV predicted by outer gap models or the pulsed curvature radiation around 50-100 GeV from millisecond pulsars predicted by polar cap models. Upper limits at this energy are also very important in constraining emission models. In summary, the next five years promise to be exciting ones for γ -ray astronomy.

References

1. R. N. Manchester et al. MNRAS **328**, 17 (2001).
2. I. A. Grenier, this proceeding, 2002.
3. L. Kuiper et al., A & A **359**, 615 (2000).
4. V. M. Malofeev, V. M. & O. I. Malov, Nature **389**, 697 (1998).
5. F. Camilo et al. ApJ **567**, L71 (2002).
6. J. P. Hughes, in prep 2002.
7. S. Murray et al., ApJ **568**, 226 (2002).
8. F. Camilo et al., ApJ , (2002), in press (astro-ph/0204219).
9. D. J. Thompson, A.K. Harding, W. Hermsen, & M.P. Ulmer, in *Proc. of the 4th Compton Symposium*, ed. C.D. Dermer, M.S. Strickman & J.D. Kurfess (AIP 410: New York,1997), 39.

10. J. K. Daugherty & A. K. Harding ApJ **458**, 278 (1996).
11. V. V. Usov & D. B. Melrose, Aust. J. Phys. **48**, 571 (1995).
12. J. Arons, ApJ **266**, 215 (1983).
13. A. G. Muslimov & A. I. Tsygan, MNRAS **255**, 61 (1992).
14. J. A. Hibschan & J. Arons, ApJ **554**, 624 (2001).
15. A. K. Harding & A. G. Muslimov, ApJ **568**, 862 (2002).
16. A. K. Harding & A. G. Muslimov, ApJ (2002), in press.
17. D. J. Thompson, in *High-Energy Gamma-Ray Astronomy* ed. F. A. Aharonian & H. J. Volk, (AIP, New York, 2001), p. 103,.
18. D. J. Thompson, et al., ApJ **436**, 229 (1994).
19. A. K. Harding, M. G. Baring & P. L. Gonthier, ApJ **476**, 246 (1997).
20. M. G. Baring & A. K. Harding, ApJ **547**, 929 (2001).
21. A. K. Harding, in *High Energy Gamma-Ray Astronomy*, , ed. F.A. Aharonian & H.J. Volk (AIP Conf. 558, New York, 2001) p. 115.
22. Q. Luo, S. Shibata & D. B. Melrose, MNRAS **318**, 943 (2000).
23. T. Bulik et al., MNRAS, **317**, 97 (2000).
24. K. S. Cheng, C. Ho & M. A. Ruderman, ApJ **300**, 500 (1986).
25. R. W. Romani, ApJ **470**, 469 (1996).
26. L. Zhang & K. S. Cheng, ApJ **487**, 370 (1997).
27. K. S. Cheng, M. A. Ruderman & L. Zhang ApJ **537**, 964 (2000).
28. K. Hirotani, ApJ **549**, 495 (2001).
29. I.-A. Yadigaroglu & R. W. Romani, ApJ **449**, 211 (1995).
30. H. I. Nel et al., ApJ **418**, 836 (1993).
31. R. W. Lessard et al., ApJ **531**, 942 (2000).
32. K. S. Cheng, in *Proc. Toward a Major Atmospheric Cherenkov Detector*, ed. T. Kifune (Tokyo: Universal Academy), 25 1994.
33. T. Yoshikoshi et al., ApJ **487**, 65 (1997).
34. K. Chen & M. A. Ruderman, ApJ **402**, 264 (1993).
35. K. Hirotani & S. Shibata, MNRAS **325**, 1228 (2001).
36. J. M. Rankin, ApJ **405**, 285 (1993).
37. A. G. Lyne & R. N. Manchester, MNRAS **234**, 477 (1988).
38. R. N. Manchester, in *Pulsars: Problems and Progress*, ed. D. B. Melrose (ASP, 1996), p. 193.
39. R. W. Romani & I.-A. Yadigaroglu, ApJ **438**, 314 (1994).
40. P. L. Gonthier et al., ApJ **565**, 482 (2002).
41. L. Zhang, Y. J. Zhang & K. S. Cheng, A & A **357**, 957 (2000).
42. A. K. Harding & B. Zhang, ApJ **548**, L37 (2001).
43. N. Gehrels et al., Nature **404**, 363 (2000).
44. I. A. Grenier & C. A. Perrot, in *Gamma2001* ed. S. Ritz et al. (AIP, New York, 2001), p. 649.
45. W. Hermsen, this proceeding 2002.
46. A. Chen, this proceeding (2002).
47. D. Smith, this proceeding (2002).